ACADEMIC PRESS

Available online at www.sciencedirect.com
SCIENCE DIRECT®

Journal of Solid State Chemistry 171 (2003) 324–328

JOURNAL OF SOLID STATE CHEMISTRY

http://elsevier.com/locate/jssc

Effect of interstitial impurities on the magnetic transitions of Er-rich Pr_xEr_{1-x} alloys ☆

K.A. Gschneidner Jr.,[a,b,*] A.O. Pecharsky,[a] Y.L. Wu,[a,b,1] and V.K. Pecharsky[a,b]

[a] *Ames Laboratory, Iowa State University, Ames, IA 50011-3020, USA*
[b] *Department of Materials Science and Engineering, Iowa State University, Ames, IA 50011-3020, USA*

Received 2 May 2002; received in revised form 26 July 2002; accepted 28 August 2002

Abstract

Interstitial impurities (primarily oxygen, but also fluorine, nitrogen, and carbon) have a considerable effect on the magnetism of Er. They lower the second-order magnetic transition temperatures (86 and 53 K), increase the first-order magnetic transition temperature (19 K) and destroy the spin-slip magnetic transition (26 K) of pure Er. Similar trends are observed in the Pr_xEr_{1-x} alloys for $0 \leqslant x \leqslant 0.4$. Pr additions to commercial-grade Er and to high-purity Er lower the two second-order and spin-slip magnetic transition temperatures, and have little or no effect on the first-order magnetic transition temperature for $x \leqslant 0.125$. The 52 and 22 K transitions are wiped out by Pr additions of $x \simeq 0.10$ and 0.02, respectively. Furthermore, the first-order transition terminates in the concentration range $0.10 \leqslant x \leqslant 0.125$, and a new magnetic phase is formed between $0.125 \leqslant x \leqslant 0.15$. For $x \simeq 0.35$, the magnetic transitions merge and for larger Pr concentrations there is only one second-order paramagnetic to antiferromagnetic transition on cooling.

Keywords: Erbium magnetic transitions; Pr–Er magnetic-phase diagram; Low-temperature heat capacity

1. Introduction

Erbium-based materials have been used as cryocooler regenerators since 1990 [1,2]. Initially, Er_3Ni has been used as the low-temperature stage regenerator to reach temperatures down to 4 K. More recently, Pr_xEr_{1-x} alloys ($0 \leqslant x \leqslant 0.5$) have been suggested as replacement cryocooler regenerator materials for lead which is the prototype material for reaching temperatures between 10 and 50 K [3]. In the latter study, the authors used a commercial grade of Er metal (~97 at% pure). In this Er metal, only three magnetic transitions were observed (84, 52, and 22 K) compared to four transitions in high-purity Er metal (86, 53, 26, and 19 K). That is, the 26 K spin-slip transition is not observed in commercial Er, and the 22 K transition in commercial Er is the same first-order magnetic transition which occurs at 19 K in high-purity Er. The addition of Pr to commercial-grade Er rapidly lowered both the 84 and 52 K transitions, but for $x \geqslant 0.05$ the 52 K transition leveled off and slightly rose until it eventually merged with the 84 K transition at 27 at% Pr. The 22 K transition temperature remained essentially constant up to 10 at% Pr, and then was lowered with further Pr additions and finally disappeared between 20 and 25 at% Pr.

In order to understand the influence of Pr on the magnetic behavior of Er, Wu et al. [4] and Moze et al. [5] reported preliminary results of dc magnetization, ac magnetic susceptibility and heat capacity [4], and neutron scattering [5] measurements using high-purity Er and Pr metals. In these studies for $0.1 \leqslant x \leqslant 0.4$ (where x is the Pr mole fraction), the 53 and 26 K transitions seem to disappear when 0.1 Pr or more is added to Er, and the 86 K transition temperature is rapidly lowered, and the 19 K transition temperature is slowly raised, such that they merge at $x \simeq 0.35$.

☆ Operated for the US Department of Energy by Iowa State University under Contract No. W-7405-ENG-82. This work was supported by the Office of Basic Energy Sciences, Materials Sciences Division.

*Corresponding author. Iowa State University, Ames Laboratory, Ames, IA 50011-3020, USA. Fax: +1-515-294-9579.

E-mail address: cagey@ameslab.gov (K.A. Gschneidner Jr.).

[1] Present address: VAW of America, Inc., 9 Aluminum Dr., Ellenville, NY 12428, USA.

0022-4596/03/$ - see front matter © 2003 Elsevier Science (USA). All rights reserved.
doi:10.1016/S0022-4596(02)00211-6

The purpose of this work is: (1) to determine the influence of small substitutions of Pr for Er (i.e., $0<x\leqslant 0.15$) on the 53 and 26 K magnetic transitions of Er; and (2) to describe and discuss the current status of our understanding of the influence of interstitial impurities on the magnetic properties of pure Er and alloys of Er doped with Pr.

2. Experimental details

Chemical analyses for both commercial and high-purity grades of Er, and high-purity Pr are given in Table 1. The commercial-grade Er (claimed to be 99.9 wt% pure) was obtained from Rhone-Poulenc. The high-purity Er and Pr starting materials were obtained from the Materials Preparation Center of the Ames Laboratory. The impurity concentration reported in Table 1 for commercial-grade Er are the average values taken from three samples of the same 1 kg batch of Er material. In general, there was a considerable variation in the reported values for the major impurities (B, C, N, O, F, Ca, La and Ta), a factor of two was common. The values reported for commercial Er and high-purity Er and Pr are based on laser ionization mass spectrometric analysis of each metal, plus wet chemical analyses for H, C, N, O, F, and Fe in both Er starting materials and Pr.

Table 1
Chemical analysis of high-purity (Ames Laboratory) erbium and praseodymium, and commercial-grade erbium[a] (in ppm atomic)

Impurity	Commercial	Ames laboratory	
	Er	Er	Pr
H	Not analyzed	994	265
B	710	1	<1
C	2000	<14	<12
N	3000	36	101
O	27,000	137	203
F	6900	220	222
Mg	14	<1	<1
Al	130	<80	30
Si	15	<8	120
Cl	29	17	44
Ca	580	3	<1
Sc	87	<1	<1
Ti	36	<1	<1
Mn	27	20	2
Fe	31	42	7
Cu	27	16	5
Y	26	3	<1
La	580	<1	<1
Dy	17	<9	<1
Ta	2000	10	7
Σ	43,210	1441	1042
Purity at%	95.7	99.86	99.89

[a] Impurities not listed are present at <10 ppm atomic level.

In both sets of the Er–Pr alloys, high-purity Pr was added to the commercial-grade Er and to the high-purity Er. Since the same Pr was added to the two different Er stocks, this was not a variable and would not account for any differences in the observed behaviors of the two sets of the Er–Pr alloys. The alloys were prepared by arc-melting ~20 g of Er + Pr on a water-cooled Cu hearth in an argon atmosphere. The samples were turned over six times and remelted to assure a homogeneous ingot for the various physical property measurements. Weight losses were less than 0.5 wt%.

The magnetic measurements were carried out using a Lake Shore magnetometer, model 7225. The ac magnetic susceptibility was measured in an ac field of 25 Oe at a frequency of 125 Hz with no bias dc field. The dc magnetization was measured over the temperature range from ~5 to ~120 K in dc fields from 0 to 50 kOe. The heat capacities at constant pressure as a function of temperature were measured using an adiabatic heat-pulse-type calorimeter [6] from ~3.5 to ~350 K in magnetic fields of 0, 20, 50, 75, and 100 kOe.

3. Results

Pure Er metal has four magnetic transitions. Two major second-order transformations occur at 86.4 K [paramagnetic (P) to a *c*-axis modulated ferromagnetic (CAM)] and at 52.7 K [CAM to a complex magnetic structure—antiphase domain + cone + helix (APD)]; a first-order transition at 19.0 K [APD to a ferromagnetic cone + helix (FC)], and one spin-slip transition at 26.2 K. The transformation temperatures for the high Pr concentration for the high-purity Pr_xEr_{1-x} alloys ($x = 0.1$, 0.2, 0.25, 0.3, and 0.4) have been reported earlier (4 and 5). Since only one ($x = 0.4$) or two ($0.1\leqslant x\leqslant 0.30$) magnetic transitions were observed in these alloys, and since there are four transitions in pure Er, we have prepared and examined four more alloys with low Pr concentrations ($x = 0.02$, 0.05, 0.125, and 0.15) to follow the 52.7 and 26.2 K transitions when diluted with Pr and which no longer exist for $x\geqslant 0.1$.

The zero magnetic field heat capacity of pure Er and $Pr_{0.02}Er_{0.98}$ are shown in Figs. 1a and b, respectively, while those of $Pr_{0.05}Er_{0.95}$, $Pr_{0.1}Er_{0.9}$, $Pr_{0.125}Er_{0.875}$, and $Pr_{0.15}Er_{0.85}$ are shown in Figs. 2a and b, 3a and b, respectively. It is quite easy to follow the effect Pr has on each of the magnetic transformations: the step-like transformation for the paramagnetic to CAM transition at 86.4 K; the sharp narrow peak for the first-order magnetic transition at 19.0 K; the modest peak for the CAM to APD transition at 52.7 K; and a slight bump at 26.2 for the spin-slip transition. It is clearly evident that Pr additions rapidly lower the paramagnetic to CAM transition (from 86.4 to ~58 K at $x = 0.15$), and slowly

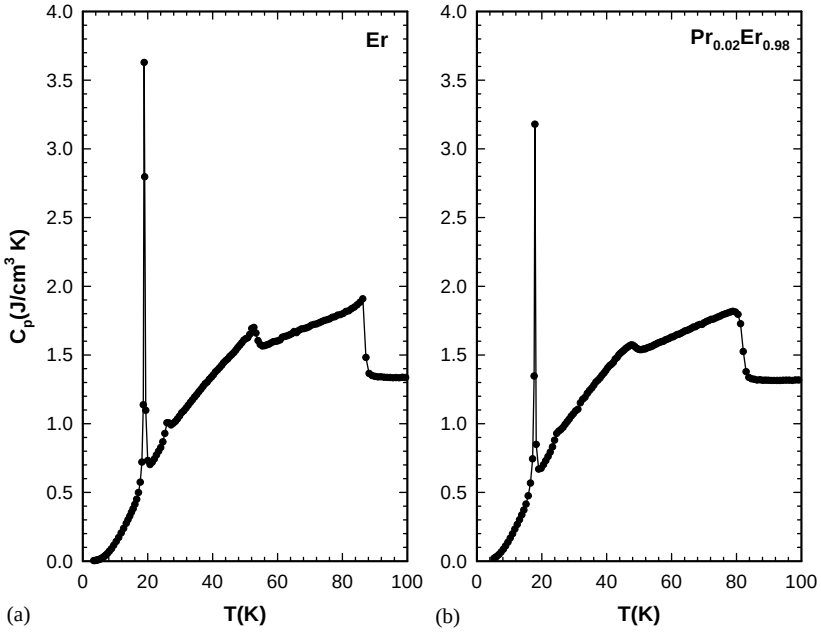

Fig. 1. Heat capacity of pure Er (a) and $Pr_{0.02}Er_{0.98}$ (b) from 0 to 100 K.

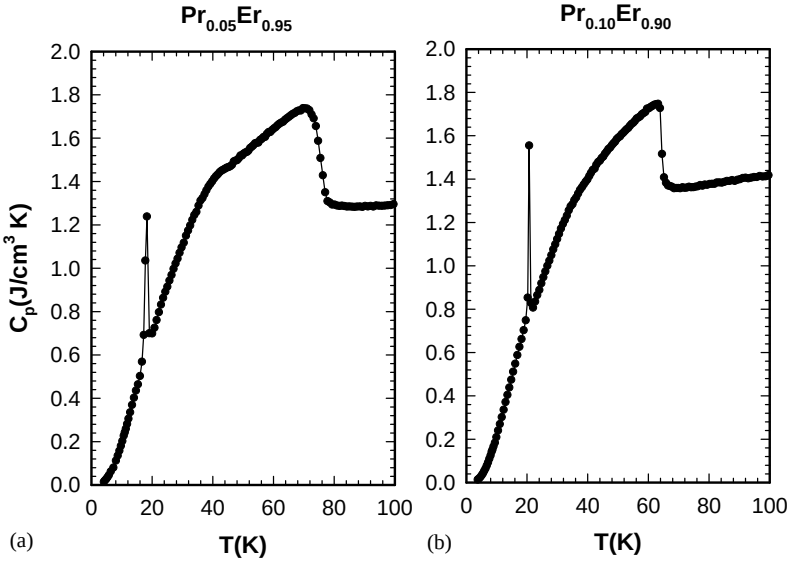

Fig. 2. Heat capacity of $Pr_{0.05}Er_{0.95}$ (a) and $Pr_{0.10}Er_{0.90}$ (b) from 0 to 100 K.

enhance the first-order transition (from 19.0 to ~22 K at $x = 0.1$). The CAM to APD transition is also rapidly lowered from 52.7 to ~35 K at $x = 0.1$ at about the same rate as the P→CAP transition (see Fig. 4). The height of this peak also decreases rapidly; it is barely discernable in $Pr_{0.10}Er_{0.90}$ (Fig. 2b), and apparently disappears between $x = 0.1$ and 0.125. The spin-slip transition temperature falls slightly from 26.2 to ~24 K for $x = 0.02$ and disappears between $0.02 \leqslant x \leqslant 0.05$. These results are summarized in Fig. 4 along with the results reported earlier for $0.1 \leqslant x \leqslant 0.4$ [4,5].

The behavior of the first-order APD→FC transition is even more interesting. As seen in Figs. 1 and 2, the sharp first-order peak is still evident up to $x = 0.10$, but at $x = 0.125$ (Fig. 3a), it basically becomes a small bump (~25 K), while a new peak seems to be developing at ~31 K. At $x = 0.15$ both peaks become stronger (Fig. 3b); the upper one (~33 K) is definitely a first-order peak for $x \leqslant 0.2$ [4]. This suggests that a new magnetic phase has formed in the Pr_xEr_{1-x} alloys for $x \leqslant 0.15$. The height of the ~25 K peak becomes smaller at $x = 0.20$ and is hardly evident at $x = 0.25$ [4].

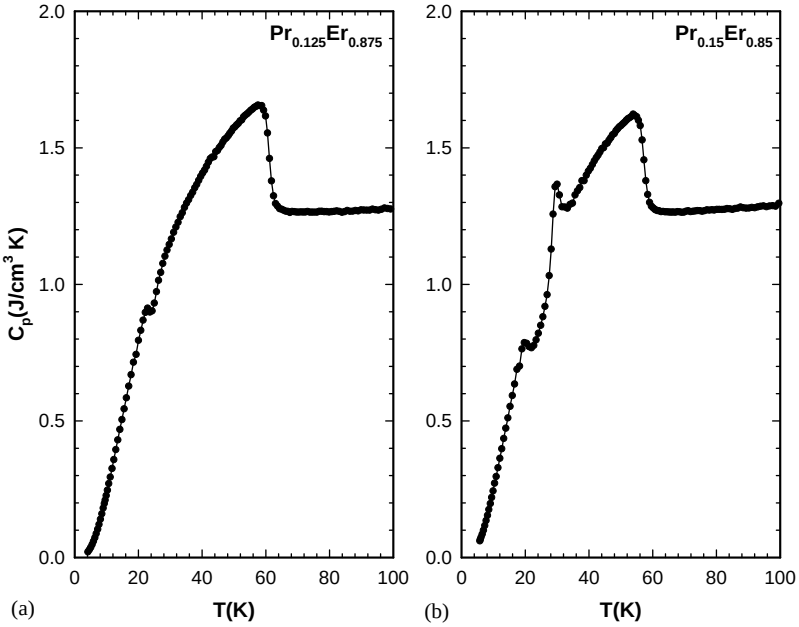

Fig. 3. Heat capacity of $Pr_{0.125}Er_{0.875}$ (a) and $Pr_{0.15}Er_{0.85}$ (b) from 0 to 100 K.

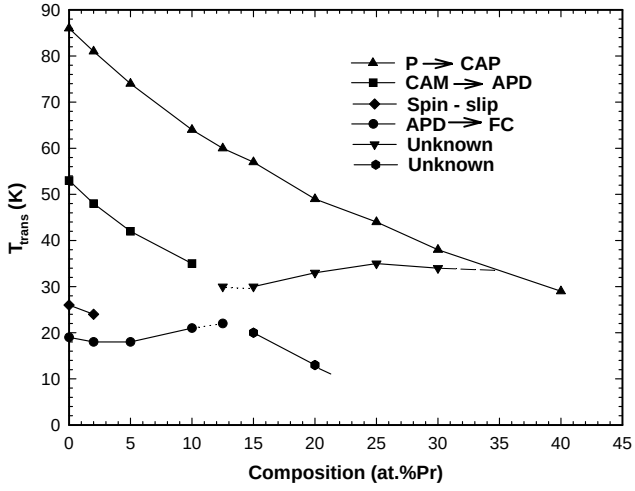

Fig. 4. Effect of Pr on the magnetic transitions of Er. The error limits for the transition temperatures are ± 1 K or less.

The magnetic field dependence of the first-order peak at ~ 33 K for $Pr_{0.20}Er_{0.80}$ is quite similar to that of the first-order peak in pure Er (19 K) [7] in that a magnetic field of ~ 20 kOe destroys the ferrimagnetic ordering process and the heat capacity peak disappears for magnetic fields greater than 20 kOe. The coercivity and remanence at 5 K of the $x = 0.20$ alloy are much larger than that of pure Er (2300 vs. 350 Oe, and 67 vs. 3 emu/g, respectively).

4. Discussion

The observed behaviors shown in Fig. 4 cannot be explained as a simple dilution effect [pure Pr orders at 0.03 K [8]]. The P→CAM transition falls off too rapidly for simple dilution, i.e., the expected T_N value from simple dilution is 60.5 for $Pr_{0.30}Er_{0.70}$ while the observed value is ~ 38 K. If one assumes that T_N scales as the de Gennes factor [0.8 for Pr and 2.55 for Er] [9], the expected T_N value is 68.6 K for the 30 at% Pr alloy which is even a larger discrepancy between the calculated and observed values than for the simple dilution. The slow rise in the first-order APD→FC transition temperature, and the disappearance of the CAM→APD and the spin-slip transitions are even more difficult to explain using such simple models.

The magnetic properties of the lanthanide metals are determined by an indirect $4f-4f$ exchange via the $6s$ conduction electrons, i.e., the Ruderman–Kittel–Kasuya–Yosida (RKKY) mechanism [9]. In a pure metal, the $6s$ electrons interact with identical ion cores in a regular periodic fashion as given by the crystal structure of the host material, in this case hcp Er. However, when an impurity atom (Pr) is introduced into the Er lattice, the ion core potential is changed in the vicinity of the impurity atom giving rise to additional scattering of the $6s$ electrons and this will affect the indirect exchange between the near neighbor $4f$ electrons. The fact that Pr also has two unpaired $4f$ electrons with an oblate $4f$ charge density compared to three unpaired $4f$ electrons with a prolate $4f$ charge density for Er [10] also plays an important role in the exchange interactions of neighboring $4f$ electrons. The role of the crystalline electric field on the $4f$ charge density will also need to be considered in a complete analysis of the influence of Pr on the magnetic phases of Er.

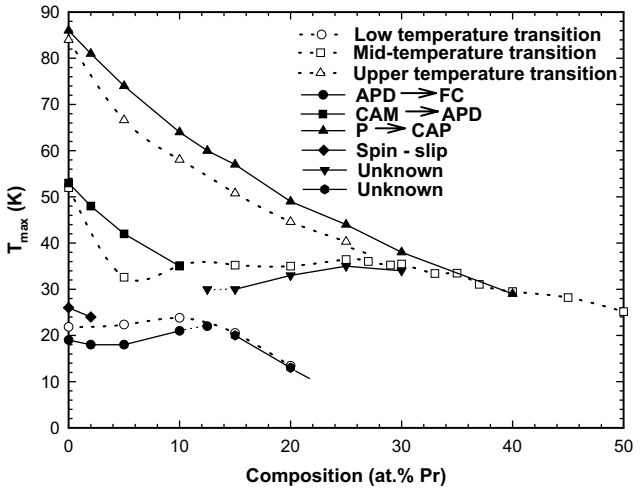

Fig. 5. The Er-rich side of the Pr–Er magnetic phase diagrams based on high-purity Er (solid points) and commercial-grade Er (open points). The error limits for the transition temperatures are ± 1 K or less.

The mediation of the de Gennes factor by these $4f$ interactions could qualitatively account for the lowering Neél (P→CAP), the CAM→APD, and spin-slip transition temperatures, especially since the rate of lowering these transition temperatures is nearly the same. However, the concentration dependence of the APD→FC transition and its disappearance for $x > 0.10$, and the existence of a new magnetic structure and its increasing ordering temperature with increasing Pr concentrations are extremely unusual and defy a reasonable explanation using conventional models. Neutron diffraction studies on these alloys are continuing and once the magnetic structures are established more quantitative theoretical analyses can be performed.

The magnetic phase diagrams of the Pr_xEr_{1-x} system based on high-purity Er (99.86 at% pure) and that based on commercial-grade Er (95.7 at% pure) are superimposed upon each other in Fig. 5. It is seen that, in general, Pr lowers the respective transition temperatures at about the same rate for commercial Er compared to high-purity Er. The general features are quite similar. Qualitatively, the presence of large amounts of interstitial impurities in commercial Er offers many more scattering sites for the $6s$ conduction electrons, which in turn decreases the indirect $4f - 4f$ interactions between neighboring magnetic atoms and thus accounts for the lower magnetic transition temperatures. However, the first-order (~ 20 K) transition does not follow this trend suggesting that the scattered $6s$ electrons enhance the ferromagnetic interactions between neighboring Er atoms, and reduce the antiferromagnetic exchange interactions. This would account for the increase in the lowest ordering ferrimagnetic temperature and the decrease in the upper antiferromagnetic order transition temperature.

References

[1] M. Sahashi, Y. Tokai, T. Kuriyama, H. Nakagome, R. Li, M. Ogawa, T. Hashimoto, Adv. Cryogen. Eng. 35 (1990) 1175.
[2] T. Kuriyama, R. Hakamada, H. Nakagome, Y. Tokai, M. Sahashi, R. Li, O. Yoshida, K. Matsumoto, T. Hashimoto, Adv. Cryogen. Eng. 35 (1990) 1261.
[3] K.A. Gschneidner Jr., A.O. Pecharsky, V.K. Pecharsky, in: R.G. Ross Jr. (Ed.), Cryocoolers 11, Kluwer Academic/Plenum Publishers, New York, 2001, p. 433.
[4] Y.L. Wu, A.O. Pecharsky, V.K. Pecharsky, K.A. Gschneidner Jr., Adv. Cryogen. Eng. 48 (2002) 3.
[5] M. Moze, W. Kockelmann, Y.L. Wu, A.O. Pecharsky, V.K. Pecharsky, K.A. Gschneidner Jr., J. Appl. Phys. 91 (2002) 8531.
[6] V.K. Pecharsky, J.O. Moorman, K.A. Gschneidner Jr., Rev. Sci. Instrum. 68 (1997) 4196.
[7] V.K. Pecharsky, K.A. Gschneidner Jr., D. Fort, Phys. Rev. B 47 (1993) 5063.
[8] K.A. McEwen, in: K.A. Gschneidner Jr., L. Eyring (Eds.), Handbook on the Physics and Chemistry of Rare Earths, Vol. 1, North-Holland, Amsterdam, 1978, p. 440.
[9] H.R. Kirchmayr, C.A. Poldy, in: K.A. Gschneidner Jr., L. Eyring (Eds.), Handbook on the Physics and Chemistry of Rare Earths, Vol. 2, North-Holland, Amsterdam, 1979, p. 59.
[10] J. Sievers, Z. Phys. B 45 (1982) 289.